EUROPEAN SYNCHROTRON RADIATION FACILITY

INSTALLATION EUROPEENNE DE RAYONNEMENT SYNCHROTRON

ESRF

Experiment Report Form

The double page inside this form is to be filled in by all users or groups of users who have had access to beam time for measurements at the ESRF.

Once completed, the report should be submitted electronically to the User Office via the User Portal:

https://wwws.esrf.fr/misapps/SMISWebClient/protected/welcome.do

Reports supporting requests for additional beam time

Reports can be submitted independently of new proposals – it is necessary simply to indicate the number of the report(s) supporting a new proposal on the proposal form.

The Review Committees reserve the right to reject new proposals from groups who have not reported on the use of beam time allocated previously.

Reports on experiments relating to long term projects

Proposers awarded beam time for a long term project are required to submit an interim report at the end of each year, irrespective of the number of shifts of beam time they have used.

Published papers

All users must give proper credit to ESRF staff members and proper mention to ESRF facilities which were essential for the results described in any ensuing publication. Further, they are obliged to send to the Joint ESRF/ ILL library the complete reference and the abstract of all papers appearing in print, and resulting from the use of the ESRF.

Should you wish to make more general comments on the experiment, please note them on the User Evaluation Form, and send both the Report and the Evaluation Form to the User Office.

Deadlines for submission of Experimental Reports

- 1st March for experiments carried out up until June of the previous year;
- 1st September for experiments carried out up until January of the same year.

Instructions for preparing your Report

- fill in a separate form for each project or series of measurements.
- type your report, in English.
- include the reference number of the proposal to which the report refers.
- make sure that the text, tables and figures fit into the space available.
- if your work is published or is in press, you may prefer to paste in the abstract, and add full reference details. If the abstract is in a language other than English, please include an English translation.

ESRF	**Experiment title:** Particle size dependent adsorption geometry of PbSe nanocrystals at the liquid-air interface	**Experiment number**: SC-4548
Beamline: ID-10	**Date of experiment**: from: 1-03-2017 to: 8-03-2017	**Date of report**: 8-9-2017
Shifts: 18	**Local contact(s)**: Oleg Konovalov	*Received at ESRF:*

Names and affiliations of applicants (* indicates experimentalists):

J.J. Geuchies* [1], E. Geraffy *[1], C. van Overbeek* [1], F. Montanarella* [1], M. Slot [1], A.V. Petukhov* [2], D.A.M. Vanmaekelbergh [1]

[1] Condensed Matter and Interfaces, Debye Institute for Nanomaterials Science, Princetonplein 1, 3584 CC Utrecht, The Netherlands

[2] Physical and Colloid Chemistry, Debye Institute for Nanomaterials Science, Padualaan 8, 3584 CH Utrecht, The Netherlands

Report:

The adsorption and self-assembly of PbSe nanocrystals (NCs) at liquid-air interfaces has led to remarkable nanocrystal superlattices, which show atomic order and a superimposed nanoscale geometry. Previous experiments [1] have unraveled the mechanism of formation of the superlattice with a square nanogeometry, which is governed by remarkable phase transitions. Following these results, we now focus on the adsorption geometry of PbSe NC monolayers at the liquid-air interface. We combine in-situ grazing-incidence small/wide angle X-ray scattering (GISAXS/GIWAXS) combined with X-ray reflectivity (XRR) to obtain the 3-D adsorption geometry of the nanocrystal monolayer. We extract the electron density profile in the direction perpendicular to the liquid-air interface from the XRR measurements, and show that nanocrystals larger than 5.5 nm align with a <100> direction perpendicular to the interface. We combine the information from the three techniques in order to build a full three-dimensional in-situ picture of PbSe nanocrystals adsorbed at the ethylene glycol-air interface. The adsorption geometry of the NCs before oriented attachment are expected to have great impact on the atomically connected 2-D superlattices.

We start the discussion of the obtained results based on the GISAXS data presented in figure 1. The data is acquired upon complete solvent evaporation. The GISAXS signal for the small NCs, shown in figure 1(a) shows Bragg rods at positions of 0.94 nm^{-1}, 1.62 nm^{-1} and 1.88 nm^{-1} in the horizontal scattering direction q_y with a FWHM of 0.06 nm^{-1}. The peak positions of 1:√3:2 indicate that the NCs are ordered in a 2-D hexagonal lattice with a NC center-to-center distance of 7.7±0.4 nm, roughly the NC diameter plus interdigitated oleic acid ligands.
The GISAXS pattern of the medium sized NCs, depicted in figure 1(b), shows Bragg rods at 0.86 nm^{-1} and 1.71 nm^{-1} in the q_y direction with a FWHM of 0.08 nm^{-1}. The 1:2 relative peak positions indicate that there is a preference for NC ordering in one dimension, e.g. the formation of linear structures. The NC center-to-center distance is calculated to be 7.3±0.7 nm. The relatively small center-to-center distance of the NCs compared to the NC diameter is not fully understood. For the large NCs, the GISAXS signal depicted in figure 1(c) shows Bragg rods at 0.75 nm^{-1}, 1.52 nm^{-1} and 2.18 nm^{-1} in the q_y direction with a FWHM of 0.05

nm^{-1}. Again, the 1:2:3 relative peak positions indicate that there is a preference for NC ordering in one dimension. The center-to-center distance is calculated to be 8.4±0.5 nm. Even though the occurrence of oriented attachment cannot be fully excluded, which would explain the decreased center-to-center distances of the NCs, we think it is highly unlikely to occur due to the presence of additional ligands in the ethylene glycol subphase.

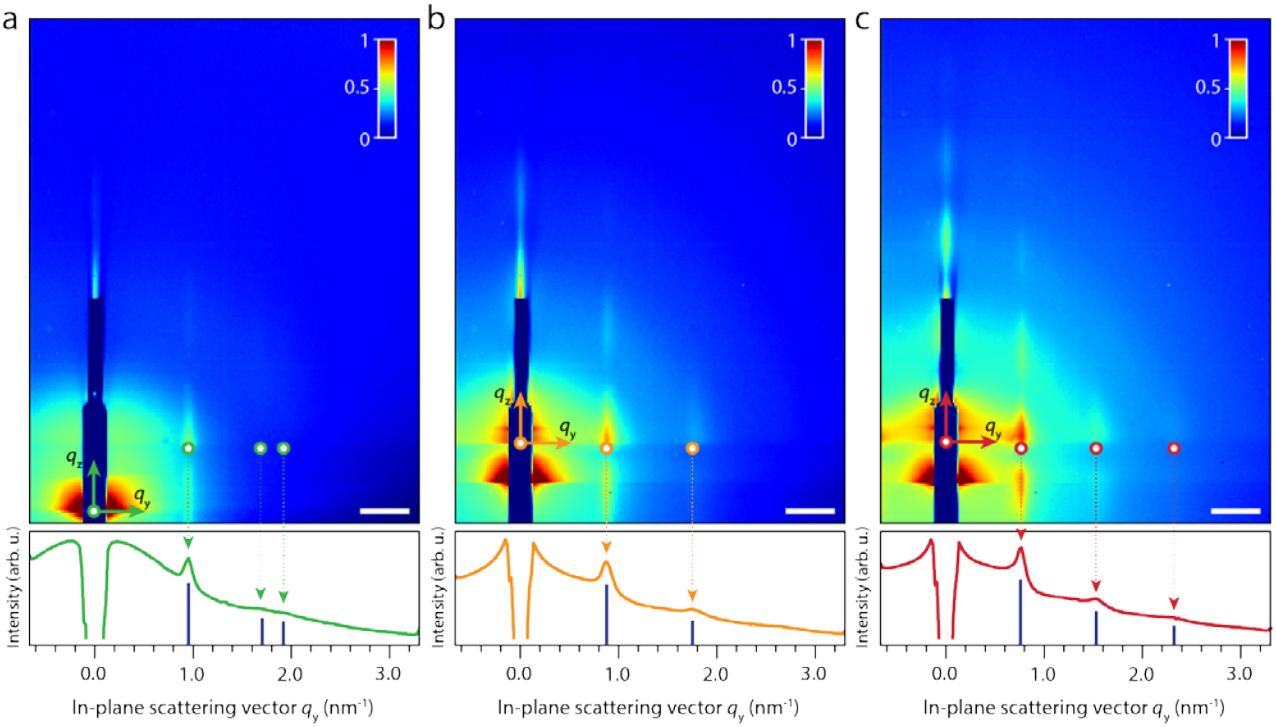

Figure 1: GISAXS data for the small (a), medium (b) and large (c) PbSe NCs.

The crystallographic orientation of the NCs is obtained by measuring the diffraction from their atomic lattices, which is presented in figure 2. We calculated the expected GIWAXS pattern for NCs having a [001] axis pointing perpendicular to the liquid-air interface in figure 2(a). Figures 2(b-d) show the GIWAXS patterns corresponding to the small, medium sized and large NCs respectively, which were recorded simultaneously with the GISAXS patterns in figure 1. For the small NCs we observe powder rings in the GIWAXS pattern, which means that the NCs do not have a preferential orientation at the liquid-air interface. Either the NCs are still freely rotatable, or the ensemble of NCs have random, static orientations which will average out in a ring in the GIWAXS pattern.

The GIWAXS pattern of the medium sized NCs, shown in figure 2(c), shows a series of well-defined diffraction spots. An azimuthal intensity trace over the reflection originating from the {222} planes shows that it has an orientation of 36.0^o with respect to the liquid-air interface, corresponding to NCs having a {001} facet pointing upwards. The FWHM of the reflection, which is an indication of the degree of rotational freedom the NCs still have at the liquid-air interface, is 6.5^o. The GIWAXS pattern of the large NCs, shown in figure 2(d), matches the calculated GIWAXS pattern very well. It shows that the NCs have the same orientation as the medium-sized NCs, i.e. a {001} facet pointing upwards. The distribution in orientations is slightly smaller, as the FWHM of the 222 reflection is 6.1^o. This means that the large NCs have less rotational freedom at the liquid-air interface.

The orientation of the NCs is also verified by looking at intensity traces in the 2θ direction along the scattering horizon (azimuthal angle equals ~1^o), which are not shown in this report. For the medium-sized and the large NCs, only reflections originating from {*hk*0} PbSe lattice planes are observed along the scattering horizon. These particular atomic planes are oriented perpendicular to the liquid-air interface when the NCs have a [001] axis pointing upwards, and hence scatter horizontally. Previously observed superlattices

from PbSe NCs have been shown to show attachment of their {100} facets. We are able to verify whether or not the NCs are attached, by looking at the FWHM of the 400 reflection in the horizontal scattering direction and estimating the crystalline size of the NCs. Since the diameters obtained using the Scherrer equation are not significantly larger than the NC diameters determined by TEM, we conclude that the NCs are not connected and no oriented attachment has occured. NC alignment was also observed by Van der Stam et al., who recently showed that upon addition of oleic acid, 11 nm polyhedral ZnS bifrustum NCs align atomically with their {002} facet pointing upwards at the ethylene glycol-air interface [2]. They show that two crystallographic orientations of the NCs are possible at the liquid-air interface. The one which is observed experimentally is determined by the relative size of the specific NC facet; the orientation is such that the facet with the largest surface area is planar with the liquid-air interface.

A similar explanation could be applied to the experiments shown here. As the NCs grow in size, the truncation is decreased and the NCs attain a more cubic shape. This means that the relative size of the {100} facets increases at the expense of the {110} and {111} facets. Especially for the large NCs, which have relatively large {100} facets, this would mean that the minima in the adsorption free energy are deeper compared to those for the other adsorption geometries. However, this does not explain why we do not observe any NCs which align crystallographically with a [111] axis perpendicular to the ethylene glycol-air interface, the alignment of the NCs for the honeycomb superlattice.

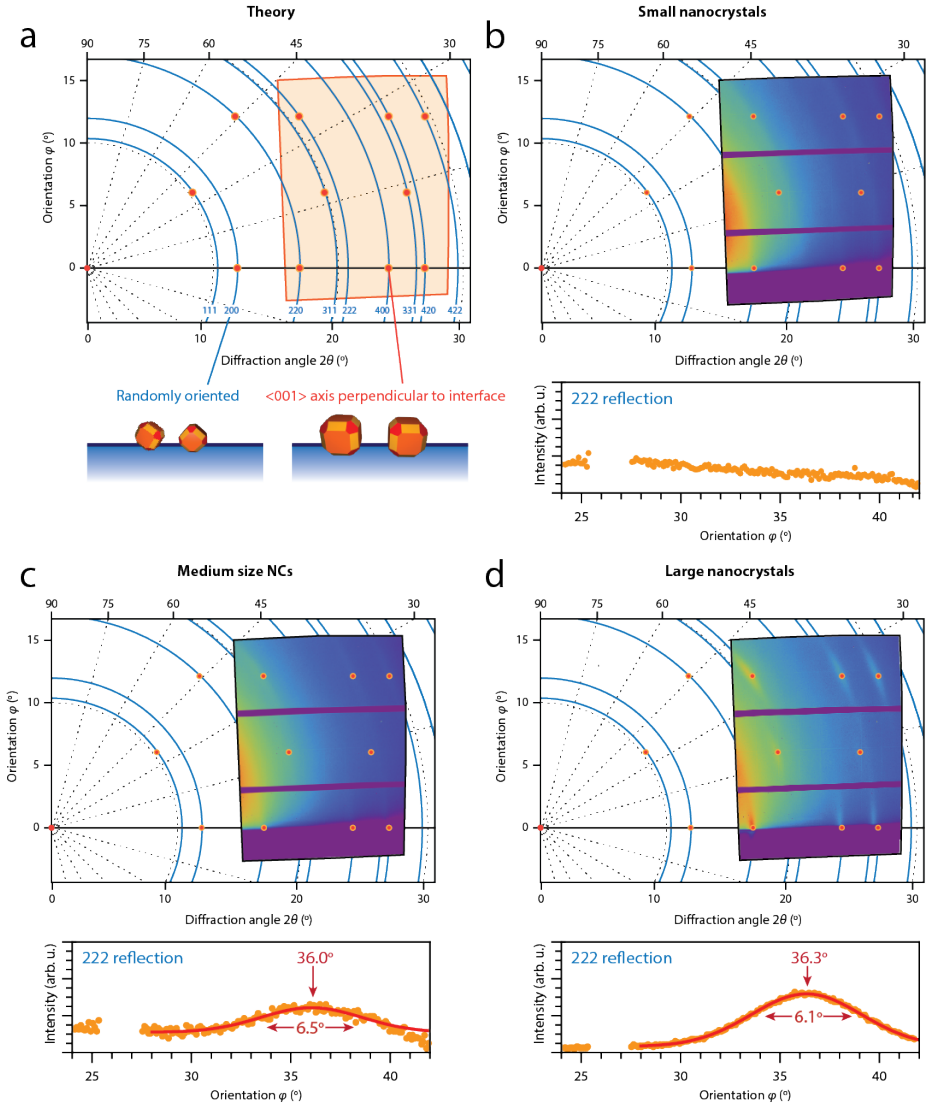

Figure 2: Analysis of the corresponding GIWAXS patterns reveal crystallographic alignment of larger PbSe NCs with respect to the liquid-air interface. Intensity traces are taken over the 222 diffraction ring vs. their azimuthal angle φ, and are shown below the image. **(a)** Calculated GIWAXS pattern for rocksalt PbSe NCs having a [001] axis perpendicular to the liquid-air interface (red dots) and when allowed full rotational freedom (blue rings). The orange area shows the position of the GIWAXS detector in this coordinate space. **(b)** GIWAXS pattern of the small NCs, showing no preferential crystallographic alignment.

(c) GIWAXS pattern of the medium-sized NCs, which can be fitted well to NCs pointing a [001] axis upwards, perpendicular to the liquid-air interface. The width of the 222 reflection is an indication of how well the NCs are atomically aligned with respect to the liquid-air interface. The medium-sized nanocrystals have a 6.5^{o} variation in orientation (FWHM). **(d)** GIWAXS pattern of the large NCs, which can also be fitted well to NCs pointing a [001] axis upwards. The width of the 222 reflection is smaller compared to the same reflection of the medium sized NCs; the large nanocrystals have a 6.1^{o} variation in orientation (FWHM).

We continue the discussion here with a comparison of the XRR data from the small and large PbSe NCs, which is presented in Figure 3. For the fitting of the data, we apply a recursive fitting procedure based on a Parratt formalism. In this fitting procedure, the nanoparticles are approximated to be spherical and are placed on an ethylene-glycol air interface. The density profile in the *z* direction is divided into *N* strata, or layers, for which the average value of the refractive index, $n_j = 1 - \delta_j + i\beta_j$, is calculated. The fit takes into account the position of the particle with respect to the liquid-air interface, the thickness of the ligand corona around the NC and several density and roughness parameters.

Figure 3 (a) shows the measured XRR curve from the small NCs as blue dots, with the corresponding fit as a red solid line. The clear oscillations of the signal only show one period, proving that we truly are looking at a monolayer of NCs. The value of the real part of the refractive index of each layer *j*, δ_j, is proportional to the electron density of that layer. This is plotted in Figure 3(b). The maximum of the SLD profile corresponds to a mean value for the center of mass of the NCs above the liquid-air interface level. The center of mass of the small NCs is sticking out 1.9 nm above the ethylene glycol-air interface. This can be rationalized considering the oleate ligands on the surface of the NCs. The apolar tails do not want to stick into the polar ethylene glycol and hence the particles prefer to be on top of the liquid. The acquired PbSe film thickness of 5.0 nm is in good agreement with the obtained size of the NCs using TEM.

Figure 3 (c) presents the measured XRR curve from the large NCs as blue dots, with the corresponding fit as a red solid line. Again only one periodicity of the XRR signal is observed, confirming that we are measuring a NC monolayer again. The corresponding SLD plot, shown in Figure 3(d) shows that the center of mass of the large NCs is sticking out 3 nm above the ethylene glycol-air interface. This also explains the easy transfer to solid substrates using a Langmuir-Schaefer type stamping technique. We do note that the models of the NCs can be improved significantly, e.g. by using a truncated cubic shape of the NCs with varying truncation parameters for the different NC sizes. This will ultimately result in better fits of the XRR data and a more detailed description of the adsorption behaviour of the NCs at the ethylene glycol-air interface. We note that the observed NC adsorption geometry could differ strongly from the initial adsorption geometry at the toluene-air interface. Future experiments will be focussed on obtaining a stable (i.e. non evaporating) toluene-air interface to see how the NCs adsorb and align during the early stages of the self-assembly-process.

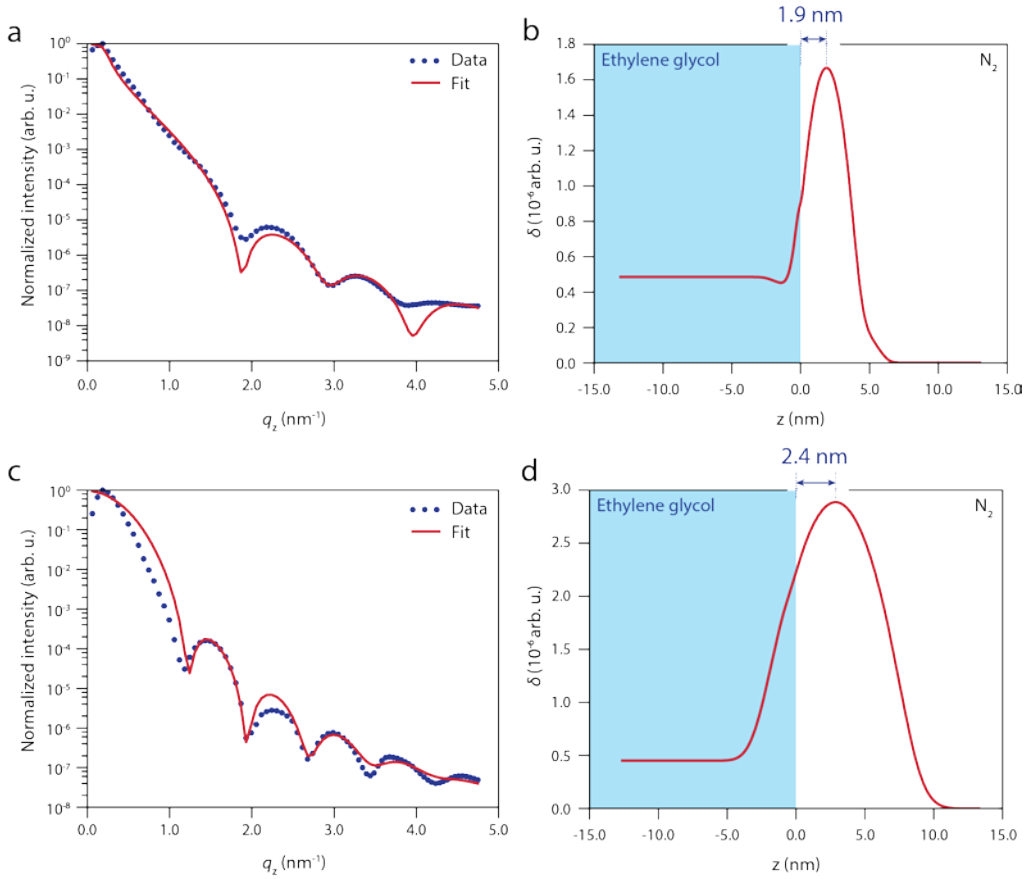

Figure 3: Analysis of the specular X-ray reflectivity of the small and large PbSe NCs. (a) Measured XRR curve from a monolayer of small PbSe NCs. The red line is the best fit of the data, in which we approximate the NCs as spherical. **(b)** Scattering length density (SLD) plot, obtained using the fitted data. The SLD is proportional to the electron density and hence gives a quantitative picture of how the nanocrystals adsorb at the liquid-air interface. The center of mass of the NCs is sticking out 1.9 nm above the ethylene glycol-air interface. **(c)** Measured XRR curve from a monolayer of large PbSe NCs. The red line is the best fit of the data. **(d)** SLD plot of the large PbSe nanocrystals, obtained using the fitted data. The center of mass of the NCs is sticking out 2.4 nm above the ethylene glycol-air interface.

The data presented above is only on three size populations of NCs. We managed to obtain data on NCs with 11 different sizes, which will allow us to do a very thorough analysis on the size-dependent adsorption geometry. For the first time, we have managed to obtain a full 3-D picture, from the NC to the atomic length scales, of how NCs adsorb at a liquid-air interface, which is of high interest to the scientific community. The remainder of the data is still being analyzed, but we aim to publish the work in a high-impact journal (e.g. ACS Nano or Nano Letters).

We would like to gratefully acknowledge dr. Oleg Konovalov for his support during the experiments and afterwards for help with the XRR analysis. He will definetely be added to the author list on our to-be paper.

[1] J.J. Geuchies et al., *Nature Materials* **2016**, 15 , pp. 1248-1254.

[2] W. van der Stam et al., *Nano Letters* **2016**, 16 (4), pp. 2608-2614.